brief communication

Phosphorylation shifts the time-dependence of cardiac Ca^{++} channel gating currents

Ira R. Josephson and N. Sperelakis
Department of Physiology and Biophysics, University of Cincinnati, College of Medicine, Cincinnati, Ohio 45267-0576 USA

ABSTRACT A general mechanism for the physiological regulation of the activity of voltage-dependent Na^+, Ca^{++}, K^+, and Cl^- channels by neurotransmitters in a variety of excitable cell types may involve a final common pathway of a cyclic AMP-dependent phosphorylation of the channel protein. The functional correlates of channel phosphorylation are known to involve a change in the probability of opening, and a negative or positive shift in the voltage dependence for activation of the conductance. The voltage dependence for activation appears to be governed by the properties of the charge movement of the voltage-sensing moiety of the channel. This study of the gating charge movement of cardiac Ca^{++} channels has revealed that isoproterenol or cAMP (via a presumed phosphorylation of the channel) speeds the kinetics of the Ca^{++} channel gating charge movement. These results suggest that the changes in the kinetics and voltage dependence of the cardiac calcium currents produced by β-adrenergic stimulation are initiated, in part, by parallel changes in the gating charge movement.

INTRODUCTION

The mechanism underlying cardiac calcium current regulation by β-adrenergic agents has been explored intensely (1–4). It has been proposed that a cyclic AMP-dependent phosphorylation of the Ca^{++} channel protein is necessary to allow the channels to open during a depolarization (3, 4). Recently, it has been reported that isoproterenol (a β-receptor agonist which increases intracellular levels of cyclic AMP and stimulates protein kinase) initiates a chain of events, leading to phosphorylation of intracellular sites on the α_1- and β-subunits of the L-type Ca^{++} channel (5). β-receptor stimulation with isoproterenol increases the macroscopic Ca^{++} current by causing an increase in the availability of functional (conducting) channels (6), and an increase in the probability of channel opening (7–9). The relationship between phosphorylation of the Ca^{++} channel and the observed changes in the single-channel current is not known, but presumably involves a conformational change of the channel protein. To further clarify the mechanism by which β-adrenergic stimulation produces alterations in cardiac Ca^{++} currents, the effects of isoproterenol were studied on the gating currents (10, 11) produced by the movement of the voltage-sensing domain(s) of the Ca^{++} channel (12–15). The gating current gives information concerning the voltage- and time-dependent conformational changes among the closed states which precede channel opening. It was found that isoproterenol speeds the turn on and decay of the gating current, especially at negative potentials. These results suggest that the physiological regulation of the voltage dependence and kinetics of the Ca^{++} current by autonomic transmitters may be related to a phosphorylation-induced alteration of the channel gating current. Some of these results have been reported elsewhere (16, 17).

METHODS

Single cell cultures were prepared from 17-d-old embryonic chick hearts by a method similar to that described previously (18). In brief, 2 dozen fertilized White Leghorn chick embryos were incubated for 17 d at 37.5°C and staged to confirm their degree of development. Hearts were sterilely removed and collected in a balanced salt solution (4°C). Tissue dissociation was accomplished by gentle rotation of the hearts in a Mg^{++}- and Ca^{++}-free Ringer solution containing 0.05% trypsin (Sigma Chemical Co., St. Louis, MO). The cell suspensions were harvested at 5-min intervals, pooled, and pelleted by centrifugation (85 *g*). The cells were washed 3 times and resuspended in tissue culture medium (M199; Gibco Laboratories, Grand Island, NY) containing 10% fetal bovine serum, and plated into 35-mm plastic petri dishes (Falcon Labware, Oxnard, CA) at a concentration of 10^5–10^6 cells/ml. The myocyte cultures were maintained at 37° and pH 7.4 in a moist-air CO_2 incubator (for 24–72 h) until used for experimentation. Single ventricular myocytes were voltage clamped using the whole cell configuration of the patch-clamp technique (19). Electrodes were fabricated from thin wall borosilicate glass (TW-150; WPI Instruments, New Haven, CT) and filled with the following solution (in millimolars): Cs^+, 120; glutamate, 120; $MgCl_2$, 2; Na_2 GTP, 0.2; Na_2 ATP, 2; EGTA, 10; Hepes buffer, 10. The pH was adjusted with Hepes to 7.25. The electrode resistances ranged from 3–8 MΩ when filled with the cesium solution. The junction potentials arising from the Cs^+ solution in the pipette, the bath solution, and the 150-mM KCl agar reference electrode were nulled before patch formation, and no further corrections were made.

The extracellular solutions contained, in millimolars: NaCl, 140; KCl, 5.4; $MgCl_2$, 1; $CaCl_2$, 1.8; glucose, 10; Hepes, 10. The pH was adjusted to 7.4. In experiments designed to examine nonlinear charge movement all ionic currents were completely blocked, using the

0006-3495/91/08/491/07 $2.00

following protocol: in addition to the internal Cs^+ solution (to block the early outward and delayed outward K^+ currents), 10 mM Cs^+ glutamate was added to the external solution (to block inward rectifier K^+ currents), 10 μM tetrodotoxin was added to block the fast Na^+ currents and $CoCl_2$ (3 mM) was added to completely block the Ca currents. Additional Ca channel blockers, such as Cd^{++} and La^{+++}, were not necessary to achieve complete blockade and their use was avoided due to the possible additional effects of these agents (voltage-dependent block and steady-state shifts in activation). The total extracellular divalent ion concentration was established before the control period, and remained constant throughout each experiment. In some experiments the Ca currents were not blocked completely so that charge movement and Ca current could be recorded simultaneously. This was accomplished by lowering the $CoCl_2$ concentration to 0.5 to 1.0 mM. The following agents were added to the bath from concentrated stock solutions (stored at 4°C): tetrodotoxin (100 μM), $CoCl_2$ (300 mM), nifedipine (100 mM) isoproterenol (100 μM), acetylcholine (1 mM). Agents (except nifedipine) were dissolved in distilled water. Nifedipine was dissolved in 100% ethanol; the final solvent concentration was $<0.1\%$ and had no effects on the charge movement.

Membrane currents were recorded using an Axopatch 1B patch clamp (Axon Instruments, Burlingame, CA). Linear capacitive current, due to the charging and discharging of the cell membrane, was suppressed by analogue capacitance compensation. Careful attention to this procedure was necessary to prevent amplifier saturation due to the initially large capacitive current signals. Data acquisition and analysis were done using the PCLAMP programs (Axon Instruments) using an IBM AT computer. Membrane currents were filtered at 10–20 KHZ and amplified 10 times with an 8-pole Bessel filter (Frequency Devices, Inc., Haverhill, MA), and digitized at 8–30 μs/pt using a 12-bit A-D converter. The voltage protocols used are shown in Fig. 1 *A*, *a*. A holding potential of −50 mV was used in all experiments to reduce (immobilize) Na^+ channel gating current (13, 15). To remove any residual linear capacitive and leakage current components, five scaled, hyperpolarizing control voltage steps (each one-fifth the amplitude of the corresponding test step) were applied from a holding potential of −100 mV (a region of linear capacitive current) and the resulting summed currents were added to the test currents. Test steps were applied 1.2 ms after returning to a common potential (usually −90 mV), which was independent of the holding potential. 4–16 responses at each potential were averaged. The entire voltage protocol was repeated at a rate of ⅓ s. The time integrals of the gating currents (charge movement) are expressed in units of nanocoulombs per microfarad of linear capacitance (nC/μF). The gating currents were blanked for a period of 250–500 μs at the onset and termination of the voltage step to minimize any residual (i.e., nonimmobilizable) Na channel gating current contribution to the charge integrals. Steady-state ON integration was performed for 6.75 ms starting at the onset of the step; OFF integration for 6.0 ms at the temination of the step. The baseline for integration was determined by the average of 40 points preceding the voltage step, or in some cases the last 40 points during the step. Because of the small magnitude of the gating currents in this preparation the variance of the noise (even after averaging) limits the resolution of the steady-state integrals to $\sim \pm 5\%$. Steady-state Q_{on}

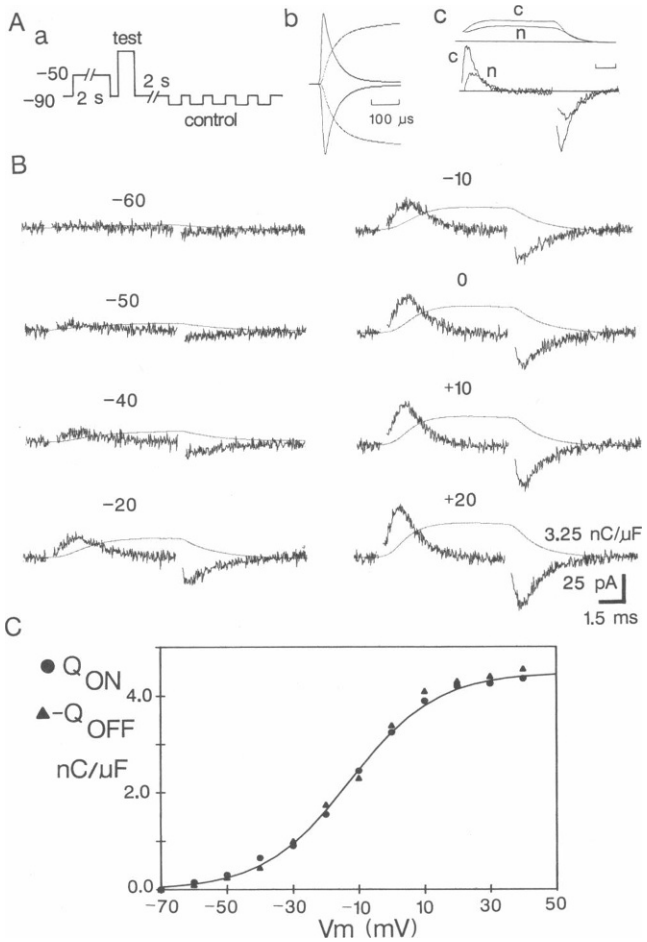

FIGURE 1 Nonlinear charge movement, recorded using a P/−5 protocol (see *A*, *a*) from embryonic chick ventricular myocytes. The time course and linearity of the control step capacity currents and their charge integrals (voltage steps from −100 to −120 mV and from −120 to −100 mV) are shown in *A*, *b*. *A*, *c* shows the nonlinear charge movement recorded using the protocol in *A*, *a* (HP −50 mV, test potential +20 mV). The current trace labeled *c* was recorded during the control period, the trace *n* was recorded 1 min after the addition of nifedipine (10^{-5} M) to the external solution (traces are superimposed, for comparison). The traces above are the superimposed charge integrals of the control and nifedipine current traces. The integration was started after the blanking period. The zero current and zero charge levels are indicated. The current, charge, and time calibrations are 10 pA, 4.0 nC/μF, and 1.5 ms. Part B shows the ON and the OFF nonlinear charge movement (*noisy traces*). Superimposed on each is the charge integral (*thin traces*) of the current. The numbers above the traces refer to the test potential (in millivolts). The holding potential was −50 mV, the subtracting holding potential during the P/−5 control steps was −100 mV. I_{Ca} was completely blocked by 3 mM $CoCl_2$. The current, charge, and time calibrations are 25 pA, 3.25 nC/μF, and 1.5 ms. The current signal was blanked for 500 μs at the beginning and ending of the test voltage step to eliminate any residual Na channel gating current from the integration. Cell capacitance, 6.5 pF. Part C is the voltage-dependence for the equilibrium ON (Q_{on}, *solid circles*), and OFF ($-Q_{off}$, *solid triangles*) Ca^{++} channel charge movement. Note that the sign of the OFF charge movement has been inverted, to allow for a comparison with the ON charge. The curve drawn through the data is the best fit to a Boltzmann expression: Q_{max}, 4.45 nC/μF; $V_{1/2}$, −12.7 mV; and V_k, 13.1 mV.

curves were best fit (nonlinear least-squares method) to a Boltzmann expression $Q_{max}/[1+\exp[-(V + V_{1/2})/V_k]]$, giving $V_{1/2}$, V_k, and Q_{max}. Shifts of the nonsteady-state (isochronal) Q_{on} vs. V_m curves were determined graphically at the $V_{1/2}$ point. Currents were digitally filtered at 3–7.5 KHZ for the figures. Experiments were conducted at 19–21°C.

RESULTS

The cultured embryonic ventricular myocyte preparation was chosen for these experiments because it offered several advantages over the adult myocyte preparation. The myocytes were small (~15 μm in diameter) and spherical, thereby permitting a fast-settling (100–200 μs) voltage clamp (see Fig. 1 *A, b*). In addition, the relative scarcity of an organized internal membrane system reduced the possibility that a fraction of the charge movement signal arose from a source other than surface membrane channels (20–22). Fig. 1 *A, c* shows the effects of the dihydropyridine Ca^{++} channel antagonist, nifedipine (10^{-5} M), on the nonlinear charge movement, using the voltage protocol shown in Fig. 1 *A, a*. Representative current traces at test potentials of +20 mV are shown (superimposed) from the control period (labeled *c*) and 1 min after the addition of nifedipine (*n*) to the external solution. A substantial reduction in the maximal amount of both the ON and OFF charge movement was produced by nifedipine (30% in this experiment, average of 33 ± 12.5% [mean ± S.D.] in three experiments) as shown by the charge integrals (superimposed above the current traces). These results, taken together with the following evidence, strongly suggest that the signal recorded using this voltage protocol is mainly composed of Ca channel charge movement.

Fig. 1 *B* shows the nonlinear charge movement, recorded using a −50 mV holding potential over a range of test potentials. Superimposed on each trace is the charge integral of that current. It is apparent that there is a close agreement between the amount of gating charge moved during depolarization (ON) and repolarization (OFF). This test substantiates that the signal is capacitive in nature. Fig. 1 *C* is a plot of the voltage dependence for the equilibrium ON (Q_{on}) and OFF ($-Q_{off}$) charge. The data display that both the ON and the OFF charge movement are a nonlinear function of potential, which saturate with increasing depolarization. The concordance of Q_{ON} and Q_{OFF} suggests that the charge movement did not immobilize during the voltage step. In some cases, however, Q_{OFF} appeared to be slightly smaller than Q_{ON} because it was not possible to separate the residual Na component from the Ca component in the OFF transient.

In addition, several other key characteristics of the nonlinear charge movement (recorded using the conditions described above) strongly suggest that it is involved with the voltage-dependent activation of L-type Ca^{++} channels. First, the charge movement is too slow to account for the activation of the Na current (23), but it precedes significant activation of the Ca^{++} current. Second, the voltage-dependence for the activation of charge movement (Fig. 1 *B*) occurs over a similar range of potentials as for the activation of L-type I_{Ca}. In comparison, the kinetically separable Na channel charge movement displays a steeper relationship, over a more negative potential range (17). Third, the amount of charge that moves during a test depolarization can be progressively reduced (immobilized) over the course of hundreds of milliseconds by application of less negative holding potentials, which also inactivate I_{Ca}. In comparison, the Na channel charge movement is partially immobilized by brief prepulses, of only a few millisecond duration. Fourth, the amount of charge moved is appropriate for the size of I_{Ca} (~100 pA) and the surface area (~700 μm^2) of these myocytes. If we estimate that there are 10 calcium channels per square micrometer (estimated from single channel experiments in this preparation), and that each channel contributes a gating charge of $4e^-$ (estimated from the slope of the Q-V curve, and assuming two independent gating particles), then the estimated charge movement is: (10 channels/μm^2) (700 μm^2/cell) ($4e^-$/channel) (1.6×10^{-19} C/e^-)/(7×10^{-12} F/cell) = 0.64 nC/μF. This value is within an order of magnitude of the experimental measurement of gating charge movement. In addition, two L-type Ca^{++} channel modulators, isoproterenol (present manuscript) and BAY K 8644 (23) act on the charge movement in a manner that correlates with the effects of these agents on I_{Ca}. Thus, the Ca^{++} channel charge movement can be characterized on the basis of its kinetics, voltage dependence and pharmacology.

Fig. 2 *A* shows the effects of isoproterenol (Iso) on both the nonlinear components of charge movement (gating current) and the L-type calcium current (I_{Ca}) recorded from an embryonic chick ventricular myocyte. In this representative experiment, I_{Ca} was isolated and reduced by ~80% (using 1 mM Co^{++}), to observe both the gating and the ionic currents simultaneously. Superimposed are the averaged currents recorded during voltage steps to −10 mV, in control conditions (*open circles*), and 2 min after exposure to Iso (10^{-6} M) (*closed circles*). Several differences are evident between the control and Iso-treated currents. The most obvious feature is that Iso produced the well-known increase in the magnitude of I_{Ca}, seen as an increase of the peak current and of the tail current after repolarization. In addition, the kinetics of activation of I_{Ca} were more rapid with Iso, resulting in a earlier time to reach peak current (8.4 ms in control, 5.5 ms for Iso, at −10 mV). The gating

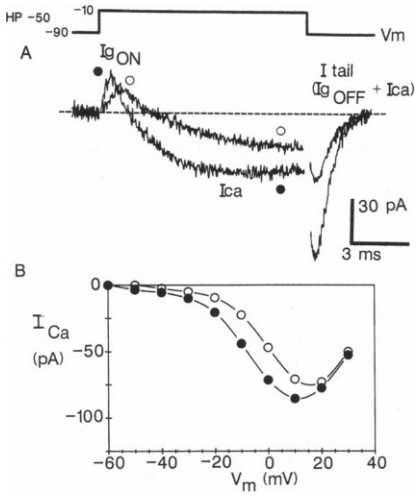

FIGURE 2 (*A*) The effects of isoproterenol (10^{-6} M) on nonlinear charge movement (gating current) and Ca^{++} currents in a cultured ventricular cell. The calcium current was partially blocked with $CoCl_2$ (1 mM). Linear ionic and capacitive currents were eliminated, as described in Methods. The current records were blanked for 250 μs. The test step voltage protocol is shown in the inset. The test potential was −10 mV, the holding potential was −50 mV. (*Open circles*) control currents; (*solid circles*) currents recorded 2 min after exposure to Iso. Cell capacitance, 6.0 pF. Each record is the average of four repetitions. (*B*) The current-voltage relationship for the peak calcium currents before (*open circles*) and after 10^{-6} M Iso (*solid circles*).

currents, which precede the inward Ca^{++} currents, were also altered by Iso, so that their time course was shifted concomitantly to result in an earlier time-to-peak and a more rapid decay phase.

The current-voltage relationship for the control (*open circles*) and Iso-stimulated (*closed circles*) peak I_{Ca} is given in Fig. 2 *B*. The enhancement of I_{Ca} by Iso has been reduced by rundown, which was accelerated by the administration of the multiple (averaged) test protocols. Increases in the peak current are apparent, however, at negative potentials, whereas there was little or no increase evident at positive potentials. This finding was confirmed in four out of a total of six additional experiments in which the peak current-voltage relationship was shifted to more negative potentials by 3–10 mV. Thus, this resulted in a voltage-dependent increase of I_{Ca} (6).

Because Iso produced effects on the charge movement which were correlated with the shifts in I_{Ca}, subsequent experiments were focussed exclusively on the Ca channel nonlinear charge movement (during complete blockade of I_{Ca}), to elucidate the nature of the alterations. Fig. 3 *A* displays the nonlinear charge movement (HP −50 mV, test potential +10 mV) before (*trace a*) and 3 min after (*trace b*) the addition of isoproterenol to the external solution. An accelation in the activation and decay of the charge movement was observed in the presence of Iso. It is important to emphasize that the contribution of Na channel charge movement in these experiments was minimized by using a conditioning holding potential (HP) of −50 mV for a 2-s duration preceding the test step. The conditioning HP immobilized at least two-thirds of the Na channel ON charge which, in this preparation, was kinetically separable from the slower, second component of Ca channel charge movement. A small, nonimmobilizable, residual component of Na channel charge movement (*arrows*) decayed rapidly (~500 μs) and was blanked out of the current records used for integration.

Fig. 3 *B* compares the time course of the gating currents (*lower panels*), and the integrals of the gating currents (*upper panels*), recorded at −10 and +10 mV, in control conditions (*a*), and after Iso (*b*). The current records have been blanked for 500 μs, and are filtered at 3 KHZ. As was suggested above, Iso accelerated both the rise and decay of the gating currents so that they peaked at earlier times, as compared with the controls. The time integrals of the currents also showed a parallel shift to earlier times.

The potential dependence of the time-to-peak, or maximum of the gating current in control conditions (*open circles*) and after Iso (*closed circles*) is shown in Fig. 3 *C*. The data points are the means (±S.E.M.) of two experiments. There was a decrease in the time-to-peak gating current (T_P) of the Iso-stimulated currents over the range of −30 to +30 mV (statistically significant at the $p < 0.005$ level). In addition, Iso accelerated the decay phase of the gating currents so that the entire distribution of charge movement occurred earlier in time.

As can be seen in Fig. 3 *B*, the control and Iso-stimulated charge integrals reached similar values during the integration periods shown. The steady-state Q_{on} vs. V_m curves differed by ±5% (within the experimental error) and were best fit to a Boltzmann expression giving the same values of $V_{1/2}$, −13.2 mV; V_k; 11.4 mV; and Q_{max}, 5.5 nC/μF (Fig. 3 *D*).

Because the Ca^{++} current peaks before the charge movement has reached a steady-state condition, it was of interest to examine the voltage dependence of the early charge movement in a nonsteady state, isochronal manner. Fig. 3 *E* shows the isochronal Q_{on} vs. V_m, integrated during the first 2 ms, for control (*open circles*) and Iso-stimulated (*closed circles*) data. During this time, the Iso-stimulated charge movement was shifted by 7 mV (at midpoint) to more negative potentials. Comparable shifts in the isochronal Q_{on} vs. V_m curves after Iso were measured in three out of a total of five other experi-

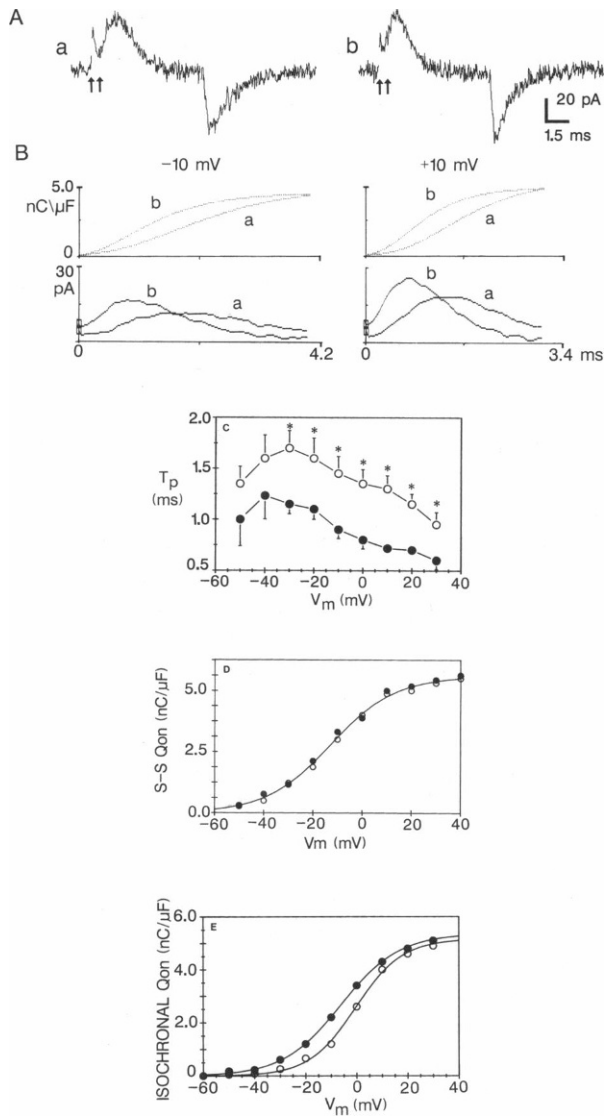

FIGURE 3 Isoproterenol shifts the time course of the calcium channel gating current. I_{Ca} was blocked completely by 3 mM $CoCl_2$. (*A*) Nonlinear charge movement (HP −50 mV, test potential +10 mV) before (*a*) and 3 min after (*b*) the addition of isoproterenol (10^{-6} M) to the external solution. The traces are displayed at a filter frequency of 7,500 Hz. The arrows denote the beginning and end of the period that is blanked out of the record for integration. During this time the residual Na channel charge movement (not immobilized by the −50 mV HP) was recorded. Time and current calibrations: 1.5 ms, 20 pA. (*B*) Representative gating current traces in control conditions (*a*), and 3 min after exposure to Iso (10^{-6} M) (*b*), are displayed for test potentials of −10 and +10 mV, using a holding potential of −50 mV. Above each set of gating currents are the charge integrals of those currents, labeled *a* for the controls, and *b* for Iso-stimulation. (*C*) The voltage-dependence of the time-to-peak (T_p) of the gating current before (*open circles*), and after Iso (10^{-6} M) (*solid circles*). Means (±S.E.M.) of three experiments. The gating current maxima were determined at 2.5 KHz with 5-point averaging, to avoid local variations due to superimposed noise. The * indicates that the group means at each voltage were statistically different at the $p < 0.005$ level (student's *t*-test). (*D*) Steady-state Q_{ON} vs. V_m relationship before (*open circles*) and after Iso (*solid circles*). The data were fit to a Boltzmann expression, as described in the text. (*E*) Isochronal (nonsteady state) Q_{on} vs. V_m curves before (*open circles*), and after Iso (*solid circles*). The current integration was performed during the first 2 ms of the depolarization. Cell capacitance, 5.5 pF. The mean shift in midpoint of four experiments was 6.25 ± 2.165 mV. The midpoint of the iso group were statistically different from the control group at the $p < 0.005$ level (student's *t*-test).

ments, and gave values ranging from −3 to −9 mV (mean ± S.D., 6.25 ± 2.165, $n = 4$).

In two experiments, the addition of 3 mM 8-bromo-cyclic AMP (a lipid soluble analogue) mimicked the effects of Iso on the gating currents (a faster activation of Q_{ON} and a negative shift of the isochronal Q_{ON} vs. V_m curve of 5 and 8 mV), suggesting that a cyclic AMP-dependent phosphorylation of the Ca^{++} channel may be a final common mechanism for both agents.

Because the increase in I_{Ca} produced by Iso is known to be reversed by acetylcholine (ACh) (18, 24), it was of importance to examine whether the effects of Iso on the gating currents could likewise be reversed by ACh. Fig. 4 shows an experiment in which a myocyte was pretreated with Iso, and the gating currents recorded. Within seconds after exposure of the myocyte to ACh (10^{-5} M) in the continued presence of the Iso, the time course of the gating currents slowed, and their peaks shifted to later times. There was no change in the series resistance compensation during these experiments or in the time course of the linear component of membrane capacity current (as judged by hyperpolarizing steps). The total

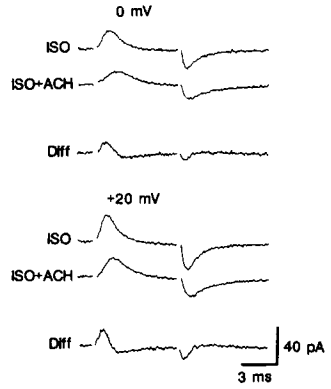

FIGURE 4 The effects of acetylcholine (ACh) (10^{-5} M) on the iso-stimulated gating current. I_{Ca} was blocked completely by 3 mM $CoCl_2$. Gating currents are shown from test potentials of 0 and +20 mV (holding potential −50 mV) after pretreatment with Iso (10^{-6} M), and 30 s after the addition of ACh (10^{-5} M), in the presence of Iso. The third trace at each potential is the difference current obtained by subtraction of the Iso + ACh current from the Iso current. Cell capacitance, Iso, 7.2 pF, Iso + ACh, 7.1 pF.

charge moved in the presence of Iso alone was approximately the same as in the presence of Iso and ACh. The shift in the time dependence of charge movement before and after the ACh antagonism of the Iso response can be seen by the difference currents, obtained by subtraction of the two traces. ACh also caused a 5-mV shift to the right (positive shift) of the Iso-treated isochronal Q_{on} curve (not shown). Similar shifts of 4 and 7 mV were observed in two other experiments.

DISCUSSION

What are the consequences of the Iso-induced shifts in the Ca^{++} gating current on I_{Ca}? If it is assumed that gating charge movement leads to channel opening, then the time course of the integral of the gating current should be related to the time course of activation of the macroscopic current. Although this assumption has not been tested rigorously (in the same cell) at present, the time course for the charge integral and for the activation of the macroscopic Ca^{++} current are similarly potential dependent. The prediction, therefore, is that Iso should speed the time to peak I_{Ca}, as confirmed here, and shorten the latency to first opening distribution for single Ca^{++} channels. Both of these effects have been reported previously (9, 26).

Furthermore, the voltage-dependent enhancement of I_{Ca} observed at more negative potentials (6) may now be explained, in part, by an earlier activation of charge movement, in combination with the other, perhaps related, effects of Iso to enhance channel availability (fewer null sweeps) and to prolong the open time (7–9). The result of these actions is that more Ca^{++} channels open earlier, at negative potentials. At more positive potentials, both the time-dependent shift in gating, as well as the effect on probability of opening, are proportionately smaller so that the Iso enhancement of I_{Ca} is not as dramatic (6).

Because Ca^{++} channels are known to open, close, and reopen during sustained depolarization, it follows that an agent which facilitates the earlier opening of channels, as well as prolongs their open times, will result in a larger macroscopic current. It should be noted that, in the steady state, Iso does not recruit significant additional charge, suggesting that an increase in channel availability may occur at a step subsequent to the initial gating charge movement. It is intriguing to speculate that at the molecular level the phosphorylation of the Ca^{++} channel domain, which results in the shift of the movement of the gating elements, also causes conformational changes which prolong the channel open state and decrease the closed dwell times. Further studies will be necessary to establish whether a relationship exists between the alterations of the gating currents and the subsequent closed and open states of the Ca^{++} channel during a maintained depolarization.

It is unlikely that the rising phase of the Ca^{++} channel gating current is the result of a bandwidth limitation of the recording system. The 10–90% decay time of the uncompensated, linear capacity current was <100–200 μs. Na^+ channel gating currents were recorded at more negative holding potentials, during the first 500 μs; they were often followed by a clear delay before the rising phase of the Ca^{++} channel gating currents (17). The presence of a rising phase of the Ca^{++} channel gating current rules out a simple two-state kinetic model (instantaneous rise, exponential fall) but would be consistent with a three- or four-closed state linear kinetic model (where the early transitions contribute little charge, or are rate limiting) or with a cooperative model (in which the transition rate constants were related to the number of charged domains of the channel already moved by the field).

Antagonism between β-adrenergic stimulation and muscarinic inhibition of I_{Ca} in cardiac muscle has been previously described (18, 24, 25), and is responsible for the classical physiological effects of autonomic neurotransmitters on the rate of beating and the force of contraction of the heart. One probable mechanism for the inhibitory effect of ACh on I_{Ca} after cyclic AMP enhancement is an inhibition of adenylate cyclase activity (25). The subsequent reduction of protein kinase activity may result in a decrease in the number of phosphorylated Ca^{++} channels. At present, the possibility of cyclic GMP (25) and/or G-protein involvement in the mediation of the ACh antagonism remains open.

It is possible that a general mechanism of regulation of ionic channels may involve a phosphorylation-dependent shift of the time and, consequently, the voltage dependence of channel gating. Additional evidence in support of this hypothesis is accumulating with respect to various types of ion channels (27), including the delayed rectifier K^+ channel (I_K) in squid axon (28). In heart, it has been reported that β-adrenergic stimulation shifts the steady-state voltage-dependence of activation of I_K and speeds its turn on (29, 30). This effect on channel gating was cAMP dependent and presumably mediated by channel phosphorylation. In addition, for Na^+ channels of brain and heart, it was found that cAMP shifts the steady-state voltage dependence of inactivation to more negative potentials (5). Thus, physiological regulation of Ca^{++}, K^+, and Na^+ channels in diverse types of excitable cells may involve channel phosphorylation at one or more sites, and may be mediated, in part, through actions on the voltage-dependent gating charge movement.

The authors gratefully thank Dr. J. Heiny for continuing advice and discussion and for providing programs for the analysis, Dr. K. Rubinson for discussion of channel chemistry, S. Osborn for preparation of the cell cultures, and Nickole Booker and Judy McMahan for typing the manuscript.

Received for publication 13 August 1990 and in final form 1 April 1991.

REFERENCES

1. Tsien, R. W., B. P. Bean, P. Hess, B. Lansman, B. Nilius, and M. C. Nowycky. 1986. Mechanisms of calcium channel modulation by beta-adrenergic agents and dihydropyridine Ca channel agonists. *J. Mol. Cell. Cardiol.* 18:691–710.
2. Trautwein, W., and D. Pelzer. 1985. Voltage dependent gating of single channels in the cardiac cell membrane and its modulation by drugs. *In* Calcium and Cell Physiology. D. Marme, editor. Springer, Berlin. 53–93.
3. Reuter, H. 1983. Calcium channel modulation by neurotransmitters, enzymes and drugs. *Nature (Lond.).* 301:569–574.
4. Sperelakis, N., and I. R. Josephson. 1989. The slow action potential and properties of the myocardial slow channels. *In* Physiology & Pathophysiology of the Heart. N. Sperelakis, editor. Martenus Nijhoff Publishing, Boston, MA. 159–186.
5. Catterall, W. A. 1988. Structure and function of voltage-sensitive ion channels. *Science (Wash. DC).* 242:50–61.
6. Bean, B. P., M. C. Nowycky, and R. W. Tsien. 1984. Beta-adrenergic modulation of calcium channels in frog ventricular heart cells. *Nature (Lond.).* 307:371–375.
7. Cachelin, A. B., J. E. dePeyer, S. Kokubun, and H. Reuter. 1983. Ca channel modulation by 8-bromo-cAMP in cultured heart cells. *Nature (Lond.).* 304:462–464.
8. Brum, G., W. Osterrieder, and W. Trautwein. 1984. Beta-adrenergic increase in the calcium conductance of cardiac myocytes studied with the patch clamp. *Pflugers Arch.* 401:111–118.
9. Yue, D. T., S. Herzig, and E. Marban. 1989. Mode 2 behavior of cardiac L-type Ca channels favored by a cAMP derivative. *Biophys. J.* 55:37*a*. (Abstr.)
10. Armstrong, C. M., and F. Bezanilla. 1973. Currents related to movement of the gating particles of the sodium channels. *Nature (Lond.).* 242:459–461.
11. Armstrong, C. M. 1981. Sodium channels and gating currents. *Physiol. Rev.* 61:644–683.
12. Field, A. C., C. Hill, and G. D. Lamb. 1988. Asymmetric charge movement and Ca currents in ventricular myocytes of neonatal rat. *J. Physiol.* 406:277–297.
13. Bean, B. P., and E. Rios. 1989. Nonlinear charge movement in mammalian cardiac ventricular cells. *J. Gen. Physiol.* 94:65–93.
14. Kostyuk, P. G., O. A. Krishtal, and V. I. Pidoplichko. 1981. Calcium inward current and related charge movement in membrane of snail neurons. *J. Physiol.* 310:403–421.
15. Hadley, R. W., and W. J. Lederer. 1989. Intramembrane charge movement in guinea-pig and rat ventricular myocytes. *J. Physiol.* 415:601–624.
16. Josephson, I. R., and N. Sperelakis. 1990. Isoproterenol shifts cardiac Ca channel gating current. *Biophys. J.* 57:305*a*. (Abstr.)
17. Josephson, I. R., and N. Sperelakis. 1991. Kinetic and voltage-dependent properties of Na and Ca channel gating currents in ventricular myocytes of embryonic chick heart. *Biophys. J.* 59:552*a*. (Abstr.)
18. Josephson, I. R., and N. Sperelakis. 1982. On the mechanism of adrenergic-cholinergic antagonism in embryonic chick cardiac muscle. *J. Gen. Physiol.* 79:69–86.
19. Hamill, O. P., A. Marty, E. Neher, B. Sakmann, and F. J. Sigworth. 1981. Improved patch-clamp techniques for high-resolution current recording from cells and cell-free membrane patches. *Pfluegers Arch. Eur. J. Physiol.* 391:85–100.
20. Moses, R. L., and F. H. Kasten. 1979. T-tubules in cultured mammalian myocardial cells. *Cell Tissue Res.* 203:173–180.
21. Cannell, M. B., J. R. Berlin, and W. J. Lederer. 1987. Effect of membrane potential changes on the calcium transient in single rat cardiac muscle cells. *Science (Wash. DC).* 238:1419–1428.
22. Cohen, N. M., and W. J. Lederer. 1988. Changes in the calcium current of rat heart ventricular myocytes during development. *J. Physiol.* 406:115–146.
23. Josephson, I. R., and N. Sperelakis. 1990. Fast activation of cardiac Ca channel gating charge by the dihydropyridine agonist, BAY K 8644. *Biophys. J.* 58:1307–1311.
24. Heschler, J., M. Kameyama, and W. Trautwein. 1986. On the mechanism of the muscarinic inhibition of the cardiac calcium current. *Pfluegers Arch. Eur. J. Physiol.* 407:182–189.
25. Hartzell, H. C. 1988. Regulation of cardiac ion channels by catecholamines, acetylcholine and second messengers. *Prog. Biophys. Mol. Biol.* 52:165–247.
26. Malecot, C. O., and W. Trautwein. 1987. On the relationship between V_{max} of slow responses and Ca-current availability in whole-cell clamped guinea pig heart cells. *Pfluegers Arch. Eur. J. Physiol.* 410:15–22.
27. Bean, B. P. 1989. Neurotransmitter inhibitions of neuronal calcium currents by changes in channel voltage dependence. *Nature (Lond.).* 340:153–156.
28. Augustine, C. K., and F. Bezanilla. 1990. Phosphorylation modulates potassium conductance and gating current of perfused giant axons of squid. *J. Gen. Physiol.* 95:245–271.
29. Giles, W., T. Nakajima, K. Ono, and E. F. Shibata. 1989. Modulation of the delayed rectifier current by isoprenaline in bull-frog atrial myocytes. *J. Physiol.* 415:233–249.
30. Duchatelle-Gourdon, I., H. C. Hartzell, and A. A. Lagrutta. 1989. Modulation of the delayed rectifier potassium current and frog cardiomyocytes by β-adrenergic agonists and magnesium. *J. Physiol.* 415:254–274.